Pressure effects on the electronic and optical properties of AWO_4 wolframites (A = Cd, Mg, Mn, and Zn): The distinctive behavior of multiferroic $MnWO_4$

J. Ruiz-Fuertes,[1,*] S. López-Moreno,[2] J. López-Solano,[3] D. Errandonea,[1] A. Segura,[1] R. Lacomba-Perales,[1] A. Muñoz,[3] S. Radescu,[3] P. Rodríguez-Hernández,[3] M. Gospodinov,[4] L. L. Nagornaya,[5] and C. Y. Tu[6]

[1]*MALTA Consolider Team. Departamento de Física Aplicada-ICMUV, Universitat de València, Burjassot, 46100 Valencia, Spain*

[2]*Facultad de Ciencias, Universidad Nacional Autónoma de México, Apdo. post. 70-646, México D. F. 04510, México*

[3]*MALTA Consolider Team. Departamento de Física Fundamental II, Instituto de Materiales y Nanotecnología, Universidad de La Laguna, La Laguna, 38205 Tenerife, Spain*

[4]*Institute of Solid State Physics, Bulgarian Academy of Sciences, 1784 Sofia, Bulgaria*

[5]*Institute of Scintillating Materials, National Academy of Sciences of Ukraine, 61001 Kharkov, Ukraine*

[6]*Fujian Institute of Research on the Structure of Matter, Chinese Academy of Sciences, Fuzhou, Fujian 350002, China*

(Received 23 May 2012; revised manuscript received 20 July 2012; published 12 September 2012)

The electronic band-structure and band-gap dependence on the d character of A^{2+} cation in AWO_4 wolframite-type oxides is investigated for different compounds (A = Mg, Zn, Cd, and Mn) by means of optical-absorption spectroscopy and first-principles density-functional calculations. High pressure is used to tune their properties up to 10 GPa by changing the bonding distances establishing electronic to structural correlations. The effect of unfilled d levels is found to produce changes in the nature of the band gap as well as its pressure dependence without structural changes. Thus, whereas Mg, Zn, and Cd, with empty or filled d electron shells, give rise to direct and wide band gaps, Mn, with a half-filled d shell, is found to have an indirect band gap that is more than 1.6 eV smaller than for the other wolframites. In addition, the band gaps of $MgWO_4$, $ZnWO_4$, and $CdWO_4$ blue-shift linearly with pressure, with a pressure coefficient of approximately 13 eV/GPa. However, the band gap of multiferroic $MnWO_4$ red-shifts at -22 meV/GPa. Finally, in $MnWO_4$, absorption bands are observed at lower energy than the band gap and followed with pressure based on the Tanabe-Sugano diagram. This study allows us to estimate the crystal-field variation with pressure for the MnO_6 complexes and how it affects their band-gap closure.

DOI: 10.1103/PhysRevB.86.125202 PACS number(s): 62.50.−p, 71.15.Mb, 78.40.Fy

I. INTRODUCTION

Tungstates of general formula AWO_4, where A is a divalent cation, are considered as the best scintillating materials for x- and γ-rays detection as well as for medical imaging applications in x-ray computed tomography.[1,2] The wide-gap semiconductors magnesium, zinc, and cadmium tungstate ($MgWO_4$, $ZnWO_4$, $CdWO_4$) are remarkable members of this family of compounds and their properties have been extensively studied during the past decade. In particular, their scintillating efficiency and radiation hardness make them prototypic scintillators for rare-event searches.[3,4] On top of that, multiferroic tungstates like manganese tungstate ($MnWO_4$) are fascinating from the fundamental-science viewpoint because of their intriguing magnetic phase diagrams.[5–8] In addition, $MnWO_4$ exhibits spontaneous ferroelectricity induced below 12.5 K. All of the above-mentioned compounds have a common monoclinic crystal structure (space group $P2/c$) named wolframite. This structure, shown in Fig. 1, consists on layers of alternating AO_6 and WO_6 octahedra that share edges forming alternating zigzag chains.[9] Despite the scintillating properties of wolframite tungstates, their long decay time is a disadvantage for several applications. Thus, tuning their electronic properties might be helpful to improve their scintillating features. However, only a few studies on their electronic properties have been reported.[4,10–12] In this context, pressure is an efficient tool to correlate changes in the interatomic distances with electronic properties. In particular, the combination of high-pressure experimental studies and band-structure calculations has been shown to be an adequate method to characterize the electronic properties of related materials like scheelite-structured tungstates.[13] Previous efforts have been carried out to understand the band structure of wolframites. Band-structure calculations have been performed in nonmagnetic $CdWO_4$ and $ZnWO_4$.[14,15] According to Refs. 14 and 15, both compounds have a direct band gap at the Z point of the Brillouin zone (see Fig. 1).[16] Additional efforts have been dedicated to studying the energy-band dispersion of the magnetic wolframites $FeWO_4$ and $CoWO_4$.[17] However, supplementary research is needed to better understand the electronic structure of magnetic and nonmagnetic wolframites.

In this work we combine high-pressure (HP) optical-absorption experiments and band-structure calculations of $MgWO_4$, $ZnWO_4$, $CdWO_4$, and $MnWO_4$. In Secs. II and III we present the experimental and computational details. In Sec. IV we first explain the opposite band-gap behavior found for $MnWO_4$ and the rest of wolframites. Then, the discussion of the pre-edge band of $MnWO_4$[18] is made on the basis of crystal-field estimations and Tanabe-Sugano (TS) diagram analysis. The two observed bands are assigned to two of the five forbidden Mn^{2+} d-d intraband transitions and their dependence with pressure as well as for the rest of d-d bands is obtained. Finally, the calculated density-of-states (DOS) and electronic band structure for wolframites at ambient pressure and 10 GPa is presented. A comparison between them elucidates the influence of Mn^{2+} $3d$ electrons in the valence band.

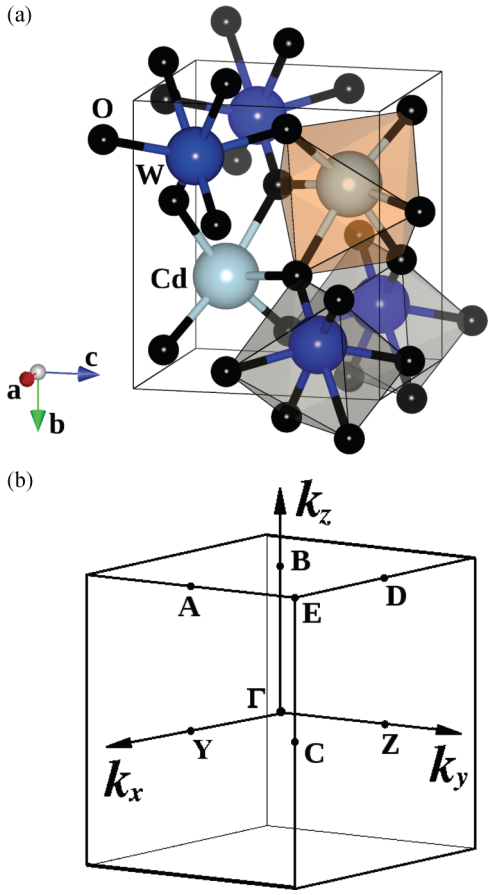

FIG. 1. (Color online) Crystal structure of $CdWO_4$ and Brillouin zone for wolframites with the highest symmetry points.

II. EXPERIMENTAL DETAILS

$MgWO_4$ crystals were prepared using the flux growth technique,[19] $ZnWO_4$ crystals were grown by means of the Czochralski method,[20] $CdWO_4$ crystals were obtained from MTI Corporation, and $MnWO_4$ crystals were grown by the high-temperature solution method.[8] Samples were cleaved from the ingots in the exfoliation (010) plane with dimensions of around (100 × 100 × 10) μm^3. They were loaded in a diamond-anvil cell (DAC) equipped by 500-μm culet IIA-type diamonds. The pressure chamber consisted in a 200-μm-diameter hole drilled in a 45-μm-thick inconel gasket. Ruby fluorescence was used as pressure standard[21] and a mixture of methanol-ethanol-water (16:3:1) was employed as pressure-transmitting medium.[22,23] Experiments were performed up to 10 GPa and a minimum of three independent experiments were carried out for each compound. At higher pressures the appearance of defects as precursors of phase transitions observed at higher pressures[19,20,24] favor the scattering of light precluding the performance of accurate optical measurements. Optical-absorption measurements in the ultraviolet-visible (UV-VIS) range under compression have been carried out making use of both a deuterium lamp as a source in the UV and a halogen one in the VIS range. Light was collimated by fused silica lenses and focused on the sample in the DAC by a confocal system consisting on a pair of Cassegrain reflecting objectives (15x) to avoid chromatic aberrations. The transmittance of the samples was measured using the sample-in sample-out method and detected with an Ocean Optics USB2000-UV-VIS spectrometer.[25]

III. CALCULATIONAL DETAILS

First-principles total-energy calculations were done within the framework of the density-functional theory (DFT)[26] and the pseudopotential method using the Vienna *ab initio* simulation package (VASP).[27] The exchange and correlation energies were taken in the generalized-gradient approximation (GGA) according to Perdew-Burke-Ernzerhof prescription.[28] The projector-augmented wave (PAW) scheme[29] was adopted and the semicore 5p electrons of W were also explicitly included in the calculations. The set of plane waves used extended up to a kinetic energy cutoff of 520 eV. This large cutoff is required to deal with the O atoms within the PAW scheme to ensure highly converged results. A dense Monkhorst-Pack (MP)[30] grid used for Brillouin-zone integrations ensures highly converged results to about 1 MeV per formula unit. We use 16 k points to perform the geometrical optimizations of these compounds with symmetry $P2/c$ and wolframite-type structure. At each selected volume, the structures were fully relaxed to their equilibrium configuration through the calculation of the forces on atoms and the stress tensor (see Ref. 31). In the relaxed equilibrium configuration, the forces are smaller than 0.004 eV/Å and the deviation in the stress tensor from a diagonal hydrostatic form is less than 1 kbar (0.1 GPa). For $MnWO_4$, we performed spin-density calculations with the GGA + U method, to take into account the strong correlation due to the d electrons of Mn, on the basis of the Dudarev's method.[32] An effective U of 3.9 eV has been used in our calculations. We found that the antiferromagnetic configuration is the most stable one.[33] The application of DFT-based total-energy calculations to the study of semiconductors properties under high pressure has been reviewed in Ref. 34, showing that the phase stability and electronic and dynamical properties of compounds under pressure are well described by DFT.

IV. RESULTS AND DISCUSSION

A. Pressure dependence of the band-gap energy

In order to determine the pressure dependence of the band gap and the absorption coefficient (α) near the band edge for the four studied wolframites, we have carried out absorption measurements in the UV-VIS-NIR region. The corresponding absorption-coefficient spectra at different pressures can be found in Figs. 2 and 3. The explored range of the absorption-coefficient values reaches around 2000–3000 cm^{-1} for all the studied compounds. The absorption-edge shape found for $MgWO_4$, $ZnWO_4$, and $CdWO_4$ is very similar to that previously reported at ambient pressure[1,35] and, given its steepness, suggests that they are direct-gap semiconductors in very good agreement with our and previous calculations.[14,15] The photon energy dependence of α for $MnWO_4$ points toward an indirect band gap, as will later be confirmed by our calculations. In Fig. 2, it can be noticed that under compression the absorption edge slightly moves to higher energies in a very similar way under compression for $MgWO_4$, $ZnWO_4$, and $CdWO_4$. In these compounds, the absorption edge exhibits an

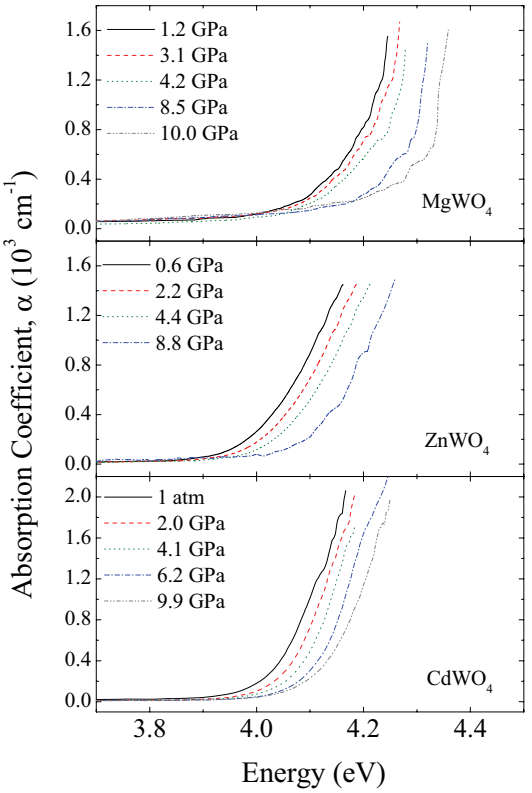

FIG. 2. (Color online) Optical-absorption spectra at different pressures up to 10 GPa for the three scintillating wolframites: $MgWO_4$, $ZnWO_4$, and $CdWO_4$.

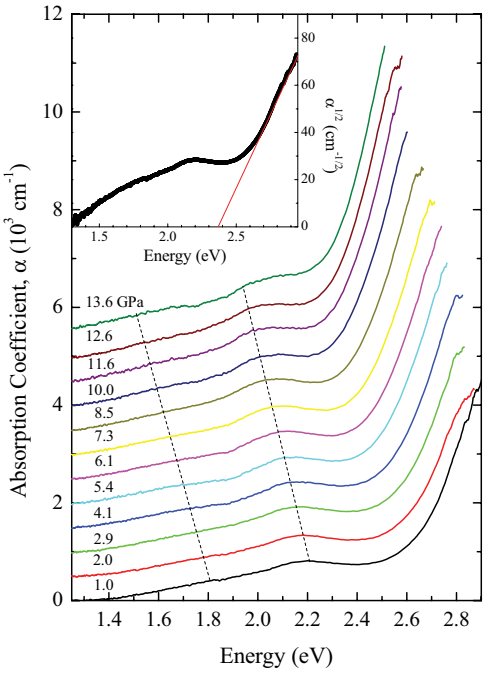

FIG. 3. (Color online) Optical-absorption spectra at different pressures for $MnWO_4$ wolframite. Spectra have been vertically shifted to facilitate the vision. In addition to the absorption-edge decrease, a red-shift movement of the two Mn^{2+} d-d transitions is observed at lower energy. (Inset) Linear dependence of the square root of the absorption spectra of $MnWO_4$. The least-squares fit of the linear portion of the absorption edge is shown as the continuous line.

exponential dependence on the photon energy, which can be understood according to Urbach's law.[36] Thus, to follow the band-gap energy (E_g) evolution with pressure, the absorption edges at different pressures have been fit according to Urbach's rule $\alpha = A_0 e^{\frac{h\nu - E_g}{E_U}}$. In this equation, E_U is related to the steepness of the absorption tail and is usually known as the Urbach's energy. $A_0 = k\sqrt{E_U}$, with k being an intrinsic constant for each material. This law has been demonstrated to work well for wolframites and related compounds.[35–38] These two parameters can be assumed to remain constant under pressure as long as the compounds remain ordered and defects are not induced by pressure.[39] As an example, for $MgWO_4$ we obtain for the whole pressure range nearly constant values of $A_0 = 500\ \mathrm{cm}^{-1}$ and $E_U = 0.095$ eV.

For $MnWO_4$, we observe that in addition to the band edge there exist two pre-edge bands. Even though the weakest one is not observed by Choi *et al.*,[18] the intense one is correctly interpreted by them as a d-d Mn^{2+} intraband transition. We shall focus on their discussion in the next subsection. Concerning the band gap of $MnWO_4$, it moves down in energy as we apply pressure (Fig. 3). As described above, the slow increase of α (with respect to the photon energy) suggests an indirect nature for the fundamental band gap. This fact is confirmed with a straight-line tendency with energy for $\alpha^{1/2} = K(h\nu - E_g)$ as can be seen in Fig. 3. In Fig. 4, we represent the variation of the band gap with pressure up to 10 GPa for the studied wolframites. For $MgWO_4$, $ZnWO_4$, and $CdWO_4$, the pressure dependence of E_g is linear, with pressure coefficients, dE_g/dP, similar to 13 meV/GPa (see Table I).

Exactly the opposite behavior is observed for $MnWO_4$, where its band gap decreases at -22 meV/GPa. In addition, in Table I we compare the present experimental and theoretical values for the band gaps at ambient pressure with previously reported values. The agreement is good within experimental accuracy.

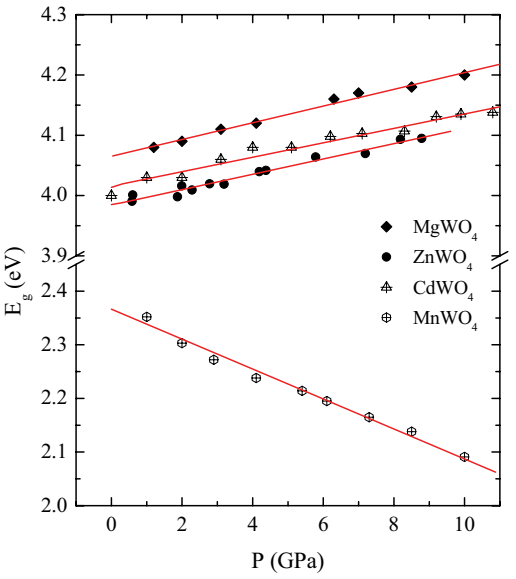

FIG. 4. (Color online) Band-gap dependence with pressure for the measured compounds. Each symbol type represents a compound and the continuous lines represent the least-square fittings to the data.

TABLE I. Previous and present experimental band gap values at ambient pressure together with calculated values. The pressure coefficients for the band gaps of the studied compounds are also shown.

	Ab initio calculations		Previous Experiments[13,34]	Present experiments	
	E_g (eV)	dE_g/dP (meV GPa^{-1})	E_g (eV)	E_g (eV)	dE_g/dP (meV GPa^{-1})
$MgWO_4$	3.22	4.52	3.9	4.06	13.9
$ZnWO_4$	2.79	−0.14	3.9	3.98	12.7
$CdWO_4$	2.91	4.60	4.2	4.02	12.0
$MnWO_4$	1.83	−28.5	2.5	2.37	−22.2

We would like to call attention to an additional fact. In the absorption spectra, in addition to the fundamental absorption, an absorption tail is also seen at lower energies. This tail is typical of orthotungstates.[35] Its nature has been the subject of considerable debate being associated to impurities or defects, but it is beyond the scope of this work. The low-energy tail overlaps partially with the fundamental absorption but it does not preclude us to the conclusions presented above. In addition, excitonic absorptions could influence the optical absorption as observed in scheelite-type $SrWO_4$.[13] In particular, the shape of the excitonic absorption can change upon compression.[40] This change can slightly influence the pressure coefficient determined for the band gap.

To conclude, we would like to comment that in oxides related to $MnWO_4$, like $PbCrO_4$,[41] with a similar pressure dependence of E_g, it has been suggested that metallization could be induced by pressure. In the case of $MnWO_4$, a linear extrapolation of E_g predicts that metallization will not take place up to 80 GPa, a pressure 50 GPa larger than the typical transition pressure of wolframites,[19,24] indicating that pressure would not induce metallization in $MnWO_4$ during the pressure stability range of the low-pressure wolframite phase.

B. Mn^{2+} *d*-electrons crystal-field splitting

As mentioned above, in $MnWO_4$ in addition to the absorption edge two weak bands can be identified at 1.83 and 2.22 eV at ambient conditions. Both bands move to lower energies following a similar trend as E_g. The band at 2.22 eV has been previously reported by Choi *et al.*[18] and interpreted as due to a Mn^{2+} *d-d* intraband transition produced by the pseudo-O_h crystal-field splitting of the Mn^{2+} *d* orbitals. The one at 1.83 eV has not been measured previously. These two bands are both spin-forbidden in a centrosymmetric system. However, the noncentrosymmetric distortions present in the MnO_6 octahedra (pseudo-O_h) favor their presence although they should be weak as observed. The measurement of only two *d-d* bands out of a total of six is not enough to unequivocally assign them. Therefore, in principle, no further information about the crystal-field ($10Dq$) or Racah parameter (B)[42,43] of $MnWO_4$ could be obtained. However, pressure happens to be an inestimable tool because it allows us to measure the bands dependence with the crystal field. According to Macavei *et al.*,[44] pressure produces a shortening of the Mn-O distances. These distances shortening should be translated into a crystal-field increase with pressure. In Fig. 5 we present the ground and first excited states of Mn^{2+} ion in a cubic octahedral O_h coordination, together with the TS diagram for the depicted transitions. We can observe for this d^5 system a spectacular spin-flip transition at $10Dq/B \approx 28$, where the system goes from a high-spin to a low-spin state. For $MnWO_4$ we start with a high-spin configuration and within our pressure range we will remain in this configuration since very large crystal fields would be required to find Mn^{2+} in low-spin configuration. In the high-spin configuration only two of the possible five accessible transitions are supposed to decrease with $10Dq$.

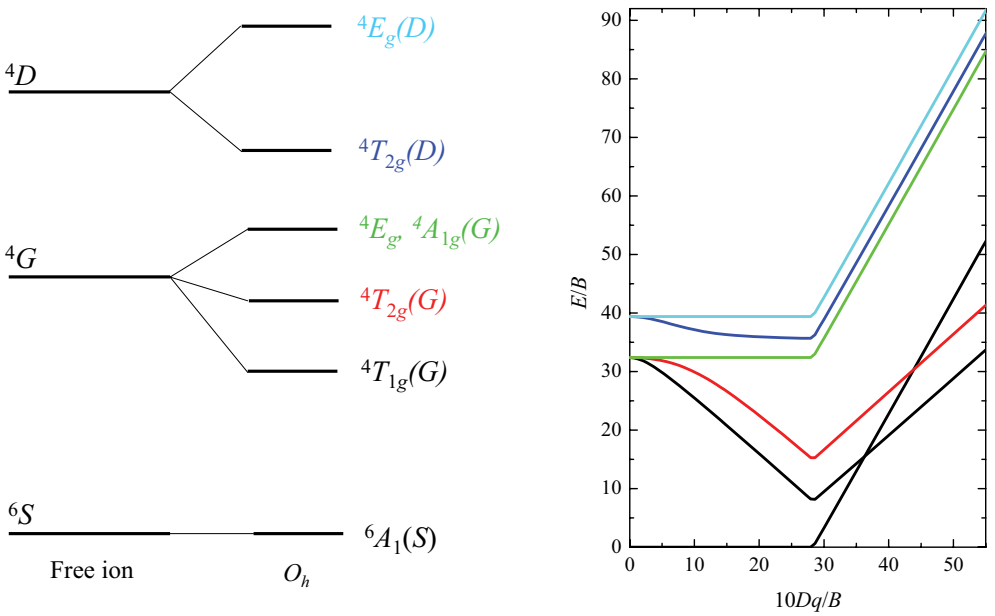

FIG. 5. (Color online) Energy-levels scheme showing the ground and excited states due to the crystal-field splitting of the Mn^{2+} d^5 levels (left). TS diagram showing the variation with the crystal field of the five electronic excited and ground states (right).

TABLE II. Mn^{2+} bands, crystal field, and Racah parameter B values at ambient pressure with their pressure coefficients.

Bands	Energy at 1 atm (eV)	$d\upsilon$,$10Dq/dP$ (meV GPa^{-1})
$^4T_{1g}(G)$	1.83	−26
$^4T_{2g}(G)$	2.22	−23
^4E_g,$^4A_{1g}(G)$	2.50	0
$^4T_{2g}(D)$	2.83	−3
$^4E_g(D)$	3.04	0
$10Dq$	0.94	27
B	0.077	—

These two ones are $^6A_1(S) \rightarrow {}^4T_{1g}(G)$ (υ_1) and $^6A_1(S) \rightarrow {}^4T_{2g}(G)$ (υ_2), with $^6A_1(S) \rightarrow {}^4T_{2g}(D)$ (υ_4) band decreasing as well but very slowly. This is exactly the type of behavior that we found for our measured bands. Assuming that the measured bands can be assigned as υ_1 and υ_2 with values at ambient pressure of $\upsilon_1 = 1.83$ eV and $\upsilon_2 = 2.22$ eV, the $\upsilon_2/\upsilon_1 = 1.22$ relative coefficient would find its correspondence in the TS diagram (Fig. 5) for $10Dq/B = 12.17$ and $\upsilon_2/B = 28.59$. Thus, the Racah parameter would have a value of $B = 0.077$ eV (see Table II) at ambient conditions. This would imply a crystal-field value of $10Dq = 0.94$ eV. These two values are in reasonable agreement with previously reported B and $10Dq$ for Mn^{2+} in MnO_6 systems, supporting our hypothesis. In fact, according to Ref. 45, for MnO_6, $0.079 < B < 0.082$ eV and $1.04 < 10Dq < 1.30$ eV. These are slightly higher values than the ones we have found for $MnWO_4$. Once both bands are identified we can follow their evolution with pressure and crystal field, thus producing our own TS diagram shown in Fig. 6. There, we can see both the experimental data and all the estimated bands from the ground state $^6A_1(S)$ to $^4T_{1g}(G)$, $^4T_{2g}(G)$, $^4E_g(G)$,$^4A_{1g}(G)$, $^4T_{2g}(D)$, and $^4E_g(D)$. For our estimations we have kept Racah parameter B constant with pressure. It is, in fact, a reasonable approximation since it has been shown for Mn^{2+} in octahedral coordination that dB/dP tends to be one order of magnitude smaller than the crystal field $10Dq$ variation with pressure $d10Dq/dP$.[45] In Table II we report the experimental and estimated band values, together with the estimated crystal field at ambient conditions and their pressure coefficients. There can be observed that the obtained pressure derivatives for n1 and n2 are much larger than those obtained previously for tetrahedrally coordinated Mn^{2+},[46] as well as happens for the crystal field. It is interesting to remark that according to the estimated pressure dependence of the crystal field, a spin crossover transition would take place for $MnWO_4$ at 47 GPa, which is a pressure larger than the transition pressure of the structural transformation known to take place at 25 GPa from Raman studies.[47]

C. Density of states

In Table III we present a comparison of the lattice parameters and atomic coordinates obtained for $MnWO_4$ at ambient pressure from x-ray diffraction experiments and from our calculations. We can observe that the calculations agree reasonably well with experiments,[44] providing a good description of the crystal structure. The pressure evolution of the structural parameters and the atomic positions also agrees

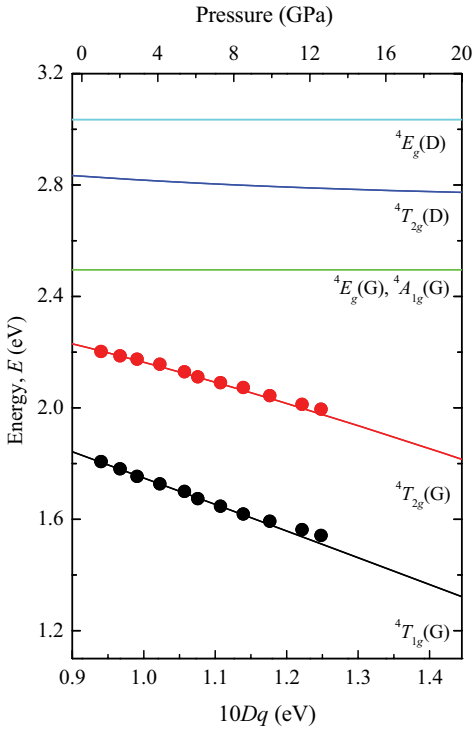

FIG. 6. (Color online) Crystal-field and pressure variation of the five Mn^{2+} bands energy. Solid dots represent the accessible experimental data obtained for the two lowest energy bands. Continuous lines represent the estimative variation of the bands derived from the experimental data.

with the experiments. The same can be affirmed for the other three wolframites here studied. Structural calculations for $CdWO_4$, $MgWO_4$, and $ZnWO_4$ have been already compared with experiments in previous works,[19,20,24,33] showing a similar agreement that for $MnWO_4$. The calculated crystal structures have been used by us to obtain the total DOS and the partial DOS projected over atoms and orbitals at different pressures in order to analyze the different contributions to the band gap evolution with pressure. We used accurate calculations to obtain the DOS and the partial DOS, with a big sampling of k points and the Gaussian smearing method with a smearing parameter of 0.05. The lm- and site-projected DOS are obtained with the method provided in the VASP package.[27] Due to the use of PAW[29] pseudopotentials, the

TABLE III. Experimental and calculated structural parameters of the wolframite $MnWO_4$.

		Experiments	Calculations
a		4.830(1) Å	4.87194 Å
b		5.7603(9) Å	5.85264 Å
c		4.994(1) Å	5.04390 Å
β		91.14(2)°	90.96061°
	Site		
Mn	$2f$	(0.5, 0.6856(4), 0.25)	(0.5, 0.67935, 0.25)
W	$2e$	(0, 0.1800(1), 0.25)	(0, 0.17737, 0.25)
O_1	$4g$	(0.211(1), 0.102(1), 0.943(1))	(0.20958, 0.10324, 0.94038)
O_2	$4g$	(0.250(1), 0.374(1), 0.393(1)	(0.25184, 0.37155, 0.39328)

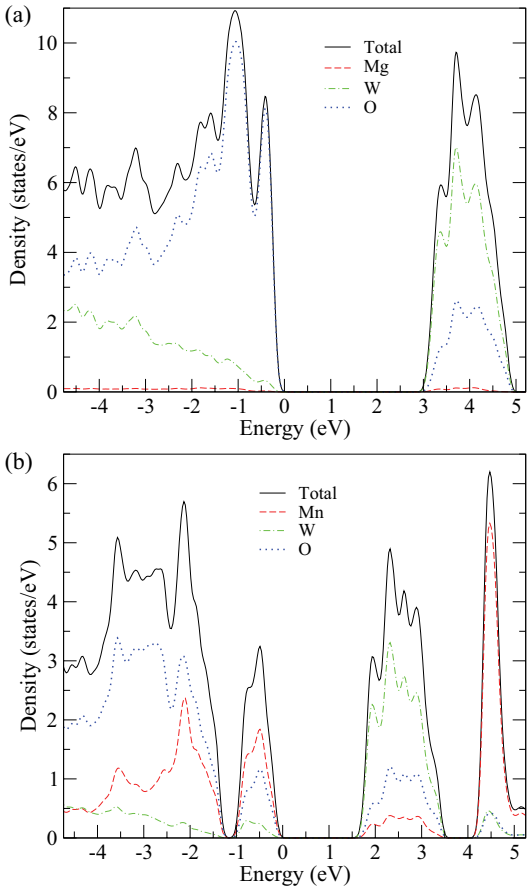

FIG. 7. (Color online) Partial density of states of $MgWO_4$ (a) and $MnWO_4$ (b) at ambient pressure.

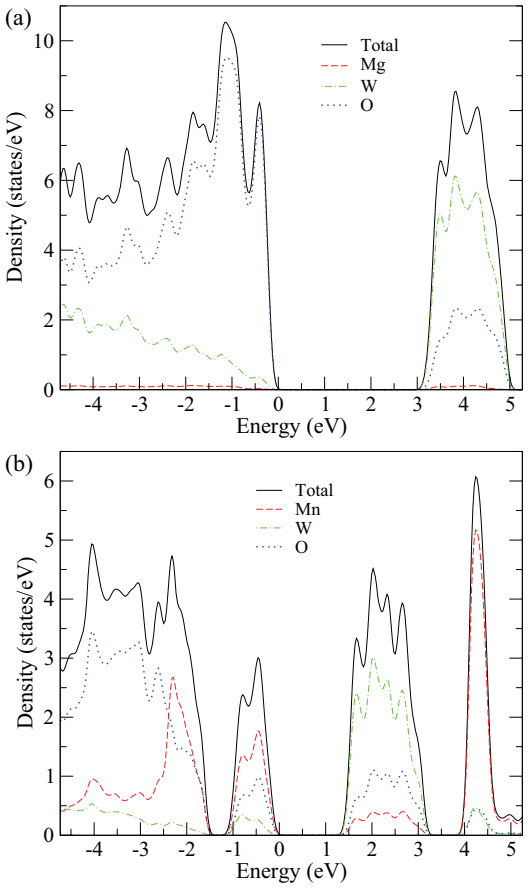

FIG. 8. (Color online) Partial density of states of $MgWO_4$ (a) and $MnWO_4$ (b) at 10 GPa.

lm- and site-projected DOS character does not require the specification of a Wigner-Seitz radius.

Figure 7 compares the partial DOS for $MgWO_4$ (a) and $MnWO_4$ (b) at ambient pressure. For $MgWO_4$ we can observe that the contribution of the Mg 3*s* states to the DOS is negligible with the upper part of the valence band being basically contributed by O 2*p* states, which are slightly hybridized with W 5*d* states, which otherwise dominate the conduction band and are slightly hybridized with the O 2*p* ones. In great agreement with previous works,[14,15] this is very similar to the DOS that we have obtained for $CdWO_4$ and $ZnWO_4$ despite the 3*d* electrons of Cd^{2+} and Zn^{2+} cations. In the former cases, the 3*d* electrons are well localized at the bottom of the valence band and only slight Cd or Zn 4*s* states hybridization with O 2*p* states takes place throughout the valence and conduction bands. Due to this similarity between the basic electronic properties of these three wolframites where the A^{2+} cation plays a small role, we will focus on the discussion of the $MgWO_4$ case in comparison to $MnWO_4$. The DOS feature observed for $MgWO_4$ at the bottom of the conduction band from 3 to 5 eV is worth discussing, since it appears in the DOS of all the wolframites at the bottom of the conduction band. It is entirely due to threefold degenerate W t_{2g} empty states produced after the splitting of the W 5*d* ones under the strong crystal field created by the surrounding six oxygen atoms, with the twofold degenerate e_g empty states being at higher energy. $MgWO_4$ DOS shows a great contrast with that of open *d*-shell wolframites as $MnWO_4$. This can be observed in Fig. 7 with the two additional features at -0.75 and 4.5 eV present in the DOS of $MnWO_4$ in comparison to $MgWO_4$. Due to the open *d*-shell character of Mn^{2+} in $MnWO_4$ the contribution from the Mn 3*d* states to both the valence and conduction bands is large, especially for the valence band. Because of the octahedral crystal field in which Mn^{2+} cations are found, and same as with W^{6+} empty 5*d* states, Mn 3*d* states are split in an e_g twofold degenerate and t_{2g} threefold degenerate state at lower energy. Thus, from -1 to 0 eV there is a two-peaks-like structure, which is basically due to the two Mn e_g states with the t_{2g} ones being found 0.5 eV below in energy, which are highly hybridized with the O 2*p* states. Additionally, the Mn 3*d* states partially contribute to the bottom of the conduction band, even though it is basically due to the W 5*d* bonding states, which are hybridized with the O 2*p* ones as happens in $MgWO_4$. In relation to the narrow DOS peak observed at 4.5 eV, it is due to the antibonding Mn t_{2g} sates. Therefore, comparing the electronic band structures of both compounds it can be stated that the fundamental transition (band gap) has to basically take place from the O 2*p* states to the W 5*d* ones in both cases, but the presence of the Mn 3*d* states, and very specially their split in the t_{2g} and e_g states, because of the crystal field, play a very important role in the band gap of $MnWO_4$. They are responsible of the band lowering of this compound.

Concerning the DOS for both compounds at 10 GPa (see Fig. 8) we can observe that on one hand, for $MgWO_4$ only

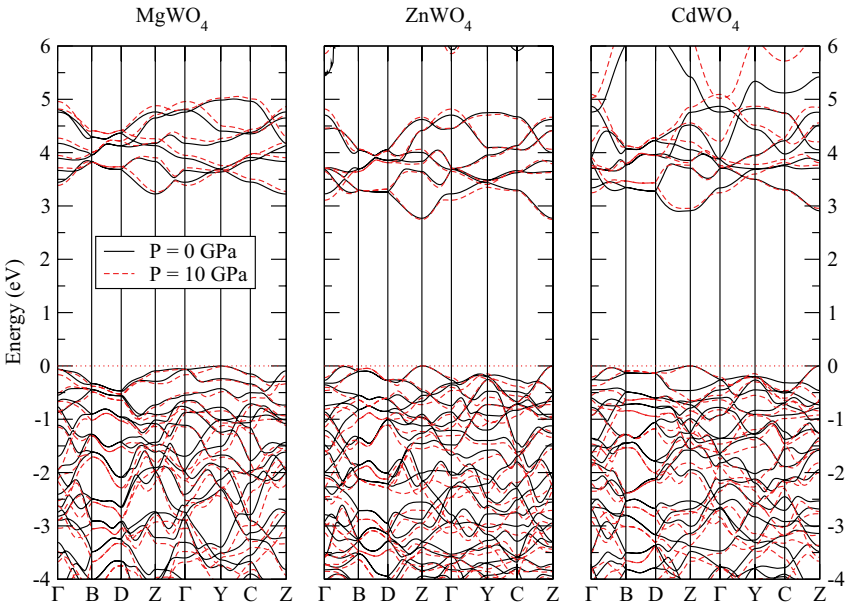

FIG. 9. (Color online) Electronic-band structure of $MgWO_4$, $ZnWO_4$, and $CdWO_4$ at ambient pressure (black) and at 10 GPa (red). The Fermi level is shown as a dotted line.

a small increase toward higher energies is observed in the conduction band, whereas on the other hand, for $MnWO_4$ pressure originates an interesting effect on its DOS. A change of the Mn 3*d* splitting is observed upon compression, which is a clear evidence of the crystal-field increase caused by the shortening of the Mn-O distances. In addition, a lowering of W t_{2g} states of the bottom part of the conduction band is induced by pressure, which has a direct effect on the band gap reduction observed. In summary, as a first approximation what occurs upon compression is that the W-dominated bottom of the conduction band moves faster than the Mn-dominated top of the valence band, causing a reduction of the band gap.

D. Energy-band dispersions

In Fig. 9 we can find the energy-band dispersion for $MgWO_4$, $CdWO_4$, and $ZnWO_4$ at ambient pressure and 10 GPa. The calculated bands for the three compounds are very similar at ambient pressure and under compression. Therefore, we will discuss here the band structure of $MgWO_4$, which has not been reported yet. As expected for materials with a conduction band with *d* character (W 5*d* in wolframites), we can state that the conduction band will be neither very dispersive nor will its energy minimum be found in the zone center. On top of that, wolframites crystallize in a monoclinic $P2/c$ space group, which is centrosymmetric. In centrosymmetric crystals, no *p*-*d* mixing takes place at the Γ point, but it does in less symmetrical points leading to upwards (downwards) dispersion in the valence (conduction) band when moving from the Γ point. This necessarily implies that in case a wolframite has a direct band gap, it has to take place away from the zone center, as can be observed for $MgWO_4$, $ZnWO_4$,[14] and $CdWO_4$,[15] with direct band gaps at the *Z* point.[16] In the case of $MgWO_4$, there is an indirect band gap very close in energy to the direct gap.

In Fig. 10 we can find the energy-band dispersion for $MnWO_4$ at ambient pressure and 10 GPa. Wolframites with unfilled *d* A^{2+} cations present indirect band gaps,[48] as expected when there is not *p*-*d* mixing in Γ but there is *p*-*d* mixing in lower symmetry points away from Γ. The *p*-*d* repulsion results in up-dispersion of the valence band and so the maximum occurs in a Brillouin-zone edge. In particular, for $MnWO_4$ we can observe that the indirect band gap takes place from the valence band top at *D* and the conduction band bottom at *Z*. We have discussed in the previous subsection that they are due to the Mn bonding e_g states, which are hybridized with the O 2*p* ones. This feature is also observed for $CuWO_4$,[49,50] with the apparition of one band at approximately -0.5 eV being the electronic band structure calculated for this compound in its antiferromagnetic state as well as with $MnWO_4$. Under high pressure, the opposite behavior is observed for $MgWO_4$ and $MnWO_4$. Whereas for $MgWO_4$ the bottom of the conduction band goes up in energy with pressure, for $MnWO_4$ the bottom of the conduction band goes down. For both compounds the

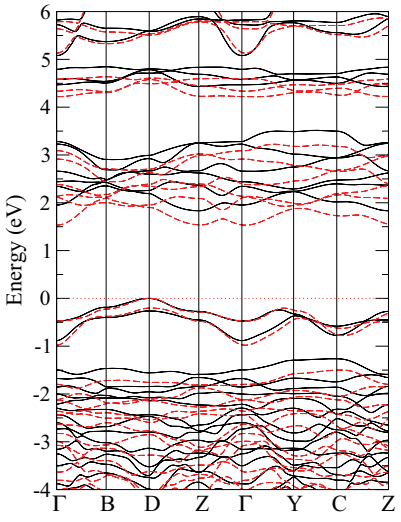

FIG. 10. (Color online) Electronic-band structure of $MnWO_4$ at ambient pressure (black) and 10 GPa (red). The Fermi level is shown as a dotted line.

top of the valence band remains at the same energy. This is translated into a band-gap increase for the $MgWO_4$ and a band-gap decrease for the $MnWO_4$, which is in agreement with the type of band-gap behavior previously reported for $CuWO_4$.[49]

It has been previously concluded that the bottom of the conduction band of orthotungstates is dominated by contributions of W $5d$ states. On the other hand, the upper part of the valence band is mainly composed by O $2p$ states. In those compounds where the valence shell of divalent cation A^{2+} contains only s or filled-d states, there is negligible contribution of them to the valence and conduction bands, but if the divalent cations have an open-d shell, a larger contribution of the metal A^{2+} to the valence and conduction bands is observed. Consequently, the decrease observed in the band gap of $MnWO_4$ upon compression can be qualitatively explained by taking into account the pressure increase of the crystal field acting on W $5d$ and O $2p$ states and the consequent increase of their hybridization with metal A^{2+} states.[51,52]

Another interesting result to be discussed is that, according to the DOS of $MnWO_4$ depicted in Figs. 7 and 8, valence and conduction band have both O $2p$ and cationic d character. In special, the valence band has mainly Mn $3d$ character. Then, the p-d interaction energy can be estimated from the splittings between the bonding and antibonding states. It happens to be of 4.5 eV at ambient pressure and 4.25 eV at 10 GPa for Mn-O bonds, which otherwise are known to compress under pressure.[44]

Finally, in Table I we present the calculated band-gap values for the four wolframites and compare both experimental and calculated values. We can observe that *ab initio* calculations, as generally happens with the GGA approximation, underestimate the values for all the wolframites in around 1 eV.[52,53] In Table I, we also present the calculated pressure coefficients. In most cases they agree reasonably well with the experimental values. In the case of $ZnWO_4$, a small negative pressure coefficient is theoretically calculated. However, the experimental coefficient is of the same magnitude but positive. Similar discrepancies have been observed in scheelite-type tungstates (e.g., $SrWO_4$).[13] They have been attributed to the possible existence of excitonic effects that are not taken into account in DFT calculations but could be strong in the absorption edge of direct semiconductors like $ZnWO_4$. A final interesting fact is that in the cases of $CdWO_4$ and $ZnWO_4$, calculations predict a band crossing at 12 GPa. Beyond this pressure, according to calculations, both materials become indirect band-gap materials with the minimum of the conduction band at D and the maximum of the valence band at Z. Unfortunately, the energy difference between the direct and indirect band gaps is smaller than 10 meV. Consequently, the band crossing cannot be detected by our experiments because it is predicted to occur at a pressure higher than the maximum pressure reached in the experiments.

V. CONCLUSIONS

High-pressure optical-absorption experiments have been performed up to a maximum pressure of 10 GPa in wolframite-type compounds $MgWO_4$, $ZnWO_4$, $CdWO_4$, and $MnWO_4$. Additionally, *ab initio* calculations have been carried out to obtain their electronic band structure and density of states at ambient pressure and 10 GPa. Experimental and theoretical results have been compared leading us to understand the influence of the A^{2+} cation in these compounds. Thus, whereas $MgWO_4$, $ZnWO_4$, and $CdWO_4$ present a direct and wide band gap, which blue-shifts with pressure at a rate of around 13 meV GPa^{-1}, multiferroic $MnWO_4$ presents an indirect and 1.6 eV smaller band gap, which red-shifts at around -22 meV GPa^{-1}. This difference in behavior for isomorphic compounds is explained in the basis of the Mn^{2+} $3d^5$ electronic levels. Mg^{2+} ($3s^2$), Zn^{2+} ($3d^{10}$), or Cd^{2+} ($4d^{10}$) with filled electronic shells do not contribute either to the uppermost of the valence band or the bottom of the conduction band, basically presenting O $2p$ character in the upmost of the valence band and W^{6+} $5d$ character at the bottom of the conduction band. However, in $MnWO_4$, Mn^{2+} ($3d^5$) contributes to the top of the valence band and the bottom of the conduction band, which translates in a reduction of the band gap in comparison to the other wolframite counterparts. Additionally, under pressure, the crystal-field increase in the MnO_6 blocks gives rise to a t_{2g}-e_g splitting increase, with a fast t_{2g} electronic levels energy decrease and a smaller e_g decrease. The same effect happens with W but in a smaller extent giving rise to a red-shift of the $MnWO_4$ band gap. Moreover, due to the important role played by Mn^{2+} d-d band in $MnWO_4$ electronic band structure, the two measurable pre-edge bands have been obtained up to 10 GPa and the remaining three bands have been estimated. This work has allowed us to obtain a crystal-field correlation with pressure and estimate that a possible spin-flip transition should not take place in $MnWO_4$. It is predicted to occur at 47 GPa, a pressure 20 GPa higher than the structural transition pressure.[47]

ACKNOWLEDGMENTS

We acknowledge the financial support from the Spanish MCYT through Grants No. MAT2010-21270-C04-01/03, No. CSD2007-00045, and No. MAT2009-14144-C03-03. J.R.-F. is indebted to the Spanish MCYT for granting an FPI fellowship (BES-2008-002043). S.L.-M. acknowledges the financial support of the UNAM of México under a postdoctoral fellowship. We thank the computer time provided by the RES (Red Española de Supercomputación) and the MALTA cluster.

*javier.ruiz-fuertes@uv.es

[1] V. B. Mikhailik and H. Kraus, Phys. Status Solidi B **247**, 1583 (2010).

[2] T. T. Monjemi, S. Rathee, D. Tu, D. W. Rickey, and B. G. Fallone, Med. Phys. **33**, 1090 (2006).

[3] V. B. Mikhailik and H. Kraus, J. Phys. D **39**, 1181 (2006).

[4] V. B. Mikhailik, H. Kraus, V. Kaputstyanyk, M. Panasyuk, Y. Prots, V. Tsybulskyi, and L. Vasylechko, J. Phys.: Condens Matter **20**, 365219 (2008).

[5]J. B. Forsyth, C. Wilkinson, and A. I. Zvyagin, J. Phys.: Condens. Matter **3**, 8433 (1991).
[6]O. Heder, N. Hollmann, I. Klassen, S. Jodlauk, L. Bohaty, P. Becker, J. A. Mydosh, T. Lorenz, and D. Khomskii, Condens. Matter. **18**, L471 (2006).
[7]K. Taniguchi, N. Abe, T. Takenobu, Y. Iwasa, and T. Arima, Phys. Rev. Lett. **97**, 097203 (2006).
[8]M. N. Iliev, M. M. Gospodinov, and A. P. Litvinchuk, Phys. Rev. B **80**, 212302 (2009).
[9]A. W. Sleight, Acta Cryst. B **28**, 2899 (1978).
[10]A. Vedda, F. Moretti, M. Fasoli, M. Nikl, and L. Laguta, Phys. Rev. B **80**, 045104 (2009).
[11]M. Fujita, M. Itoh, T. Katagiri, D. Iri, M. Kitaura, and V. B. Mikhailik, Phys. Rev. B **77**, 155118 (2008).
[12]M. Kirm, V. Nagirnyi, E. Feldbach, M. De Grazia, B. Carré, H. Merdji, S. Guizard, G. Geoffroy, J. Gaudin, N. Fedorov, P. Martin, A. Vasil'ev, and A. Beldky, Phys. Rev B **79**, 233103 (2009).
[13]R. Lacomba-Perales, D. Errandonea, A. Segura, J. Ruiz-Fuertes, P. Rodríguez-Hernández, S. Radescu, J. López-Solano, A. Mújica, and A. Muñoz, J. Appl. Phys. **110**, 043703 (2011).
[14]Y. Abraham, N. A. W. Holzwarth, and R. T. Williams, Phys. Rev. B **62**, 1733 (2000).
[15]A. Kalinko, A. Kuzmina, R. A. Evarestov, Solid State Commun. **149**, 425 (2009).
[16]In order to avoid confusion we would like to comment that we have used in this work the Brillouin zone defined in the most updated crystallographic tables (http://www.cryst.ehu.es/cryst/get_kvec.html). Note that our Brillouin zone has been drawn using a different setting than the one used previously by some authors.[14] In particular, the old Y point of the Brillouin zone becomes the Z point in our nomenclature. The readers should pay special attention when comparing the different calculated band structures to avoid misunderstandings.
[17]S. Rajagopal, V. L. Bekenev, D. Nataraj, D. Mangalaraj, and O. Y. Khyzhun, J. Alloys Compd. **496**, 61 (2010).
[18]W. S. Choi, K. Taniguchi, S. J. Moon, S. S. A. Seo, T. Arima, H. Hoang, I. − S. Yang, T. W. Noh, and Y. S. Lee, Phys. Rev. B **81**, 205111 (2010).
[19]J. Ruiz-Fuertes, D. Errandonea, S. López-Moreno, J. González, O. Gomis, R. Vilaplana, F.J. Manjón, A. Muñoz, P. Rodriiguez-Hernández, A. Friedrich, I. A. Tupitsyna, and L. L. Nagornaya, Phys Rev. B **83**, 214112 (2011).
[20]D. Errandonea, F. J. Manjón, N. Garro, P. Rodríguez-Hernández, S. Radescu, A. Mújica, A. Muñoz, C. Y. Tu, Phys. Rev. B **78**, 054116 (2008).
[21]H. K. Mao, P. Bell, J. Shaner, and D. Steinberg, J. Appl. Phys. **49**, 3276 (1978).
[22]S. Klotz, J. C. Chervin, P. Munsch, and G. Le Marchand, J. Phys. D: Appl. Phys. **42**, 075413 (2009).
[23]D. Errandonea, Y. Meng, M. Somayazulu, and D. Häusermann, Physica B **355**, 116 (2005).
[24]R. Lacomba-Perales, D. Errandonea, D. Martínez-García, P. Rodríguez-Hernández, S. Radescu, A. Mújica, A. Muñoz, J. C. Chervin, and A. Polian, Phys. Rev. B **79**, 094105 (2009).
[25]A. Segura, J. A. Sans, D. Errandonea, D. Martinez-García, and V. Fages, Appl. Phys. Lett. **88**, 011910 (2006).
[26]P. Hohenberg and W. Kohn, Phys. Rev. **136**, B864 (1964).
[27]G. Kresse and J. Hafner, Phys. Rev. B **47**, 558 (1993); **49**, 14251 (1994); Comput. Mat. Sci. **6**, 15 (1996); Phys. Rev. B **54**, 11169 (1996).
[28]J. Perdew, K. Burke, and M. Ernzerhof, Phys. Rev. Lett. **78**, 1396 (1997)
[29]P. E. Blöchl, Phys. Rev. B **50**, 17953 (1994); G. Kresse and D. Joubert, *ibid*. **59**, 1758 (1999).
[30]H. J. Monkhorst and J. D. Pack, Phys. Rev. B **13**, 5188 (1976).
[31]F. J. Manjón, D. Errandonea, N. Garro, J. Pellicer-Porres, P. Rodríguez- Hernández, S. Radescu, J. López-Solano, A. Mujica, and A. Muñoz, Phys. Rev. B **74**, 144111 (2006).
[32]S.L. Dudarev, G. A. Botton, S. Y. Savrasov, C. J. Humphreys, and A. P. Sutton, Phys. Rev. B **57**, 1505 (1998).
[33]J. Ruiz-Fuertes, S. López-Moreno, D. Errandonea, J. Pellicer-Porres, R. Lacomba-Perales, A. Segura, P. Rodríguez-Hernández, A. Muñoz, A. H. Romero, and J. González, J. Appl. Phys. **107**, 083506 (2010).
[34]A. Mujica, A. Rubio, A. Muñoz, and R. J. Needs, Rev. Mod. Phys. **79**, 863 (2003).
[35]R. Lacomba-Perales, J. Ruiz-Fuertes, D. Errandonea, D. Martınez-Garcıa, and A. Segura, Europhys. Lett. **83**, 37002 (2008).
[36]F. Urbach, Phys. Rev. **92**, 1324 (1953).
[37]R. Lacomba-Perales, D. Errandonea, A. Segura, J. Ruiz-Fuertes, P. Rodríguez-Hernández, S. Radescu, J. López-Solano, A. Mújica, and A. Muñoz, J. Appl. Phys. **110**, 043703 (2011).
[38]M. Itoh, H. Yokota, M. Horimoto, M. Fujita, and Y. Usuki, Phys. Status Solidi B **231**, 595 (2002).
[39]J. Ruiz-Fuertes, D. Errandonea, F. J. Manjón, D. Martínez-García, A. Segura, V. V. Ursaki, and I. M. Tiginyanu, J. Appl. Phys. **103**, 063710 (2008).
[40]S. Gilliland, J. Pellicer-Porres, A. Segura, A. Muñoz, P. Rodríguez-Hernández, D. Kim, M. Lee, and T. Kim, Phys. Status Solidi B **244**, 309 (2007).
[41]E. Bandiello, D. Errandonea, D. Martinez-Garcia, D. Santamaria-Perez, and F. J. Manjon, Phys. Rev. B **85**, 024108 (2012).
[42]G. Racah, Phys. Rev. **62**, 438 (1942).
[43]Y. Tanabe and S. Sugano, J. Phys. Soc. Jpn. **11**, 864 (1956); **9**, 766 (1954); **9**, 753 (1954).
[44]J. Macavei and H. Schulz, Z. Kristallogr. **207**, 193 (1993).
[45]U. Hålenius, F. Bosi, and H. Skogby, Am. Mineral. **92**, 1225 (2007).
[46]Y. Rodríguez-Lazcano, L. Nataf, and F. Rodríguez, Phys. Rev. B **80**, 085115 (2009).
[47]J. Ruiz-Fuertes (private communication, 2012).
[48]V. V. Atuchin, I. B. Troitskaia, O. Y. Khyzhun, V. L. Bekenev, and Y. M. Solonin, Int. J. Appl. Phys. Math. **1**, 19 (2011).
[49]J. Ruiz-Fuertes, D. Errandonea, A. Segura, F. J. Manjón, Zh. Zhuc, C. Y. Tu, High Press. Res. **28**, 565 (2008).
[50]J. Ruiz-Fuertes, A. Segura, F. Rodrıguez, D. Errandonea, and M. N. Sanz-Ortiz, Phys. Rev. Lett. **108**, 166402 (2012).
[51]D. Errandonea, D. Martínez-García, R. Lacomba-Perales, J. Ruiz-Fuertes, and A. Segura, Appl. Phys. Lett. **89**, 091913 (2006).
[52]S. Lopez-Moreno, P. Rodrıguez-Hernandez, A. Muñoz, A. H. Romero, and D. Errandonea, Phys. Rev. B **84**, 064108 (2011).
[53]V. Panchal, D. Errandonea, A. Segura, P. Rodriguez-Hernandez, A. Muñoz, S. Lopez-Moreno, and M. Bettinelli, J. Appl. Phys. **110**, 043723 (2011).